DOI: 10.1002/ejic.200801037

One-Step Synthesis and Characterization of SiC, Mo_2C, and WC Nanostructures

Vilas G. Pol,*[a,b] Swati V. Pol,[a,b] and Aharon Gedanken[a]

Keywords: Carbides / Synthesis design / Nanotubes / Nanorods / High-surface-area materials

This review describes a novel approach for the syntheses of various carbides of silicon, tungsten, and molybdenum at a relatively low temperature by using the RAPET (Reactions under Autogenic Pressure at Elevated Temperature) process. The solvent-, template-free and straightforward RAPET process was used to synthesize a range of new carbide materials with or without the use of catalysts. The thermolysis of precursor(s) in a closed reactor without using additional reducing gases and the characterization of the obtained high-surface-area β-SiC nanorods, micro- or nanosized Mo_2C spheres and WC nanotubes are the key issues described. The capability of the RAPET process to fabricate nanoparticles, nanorods, and nanotubes of different carbides in a single-step reaction is also demonstrated. By taking advantage of the achieved highest surface area (563 m^2/g) of SiC, it was possible to store approximately 2 wt.-% of H_2 at room temperature and 6 MPa.

Introduction

Carbides of silicon, tungsten, and molybdenum are attractive materials due to their outstanding physical and chemical properties, such as high thermal conductivity, resistance towards oxidation, mechanical strength, and chemical inertness.[1] Various carbides have numerous applications in different fields such as biomaterials,[1] semiconducting devices,[2] lightweight/high-strength structures,[3] and high-temperature-resistant materials.[4] It is also found that the catalytic properties of carbides strongly depend on their surface structure and composition, which are closely associated with their preparation methods.[5] Taking into account the influence of the size, shape, and texture of the SiC nanomaterials on their properties, a few reports on the synthesis of SiC are highlighted here. The synthesis of SiC nanoparticles[6] is carried out by employing arc-plasma processing, nanowires[7] are prepared by using the carbothermal reduction process, and nanorods[8] are made by ball milling the precursors followed by heating at 1200 °C under an atmosphere of argon gas. Ultrafine SiC with a 150 m^2/g surface[9] area, SiC nanotubes,[10] and hollow nanospheres[11] are also reported. There are several routes for preparing WC, including the direct carburization of tungsten powder, solid-state metathesis, reduction carburization, mechanical milling, and polymeric precursor routes using metal alkoxides.[12,13] WC production generally proceeds as a two-step process. First, the oxide is reduced to high-purity tungsten in an atmosphere of hydrogen. The tungsten metal is then mixed with the required amount of carbon and reacts at a temperature of 1400–1600 °C to produce WC.[14,15] Mo_2C is produced by methods such as gas phase reactions of volatile metal compounds, reaction of gaseous reagents with solid-state metal compounds, pyrolysis of metal complexes, carbothermal hydrogen reduction,[16] and solution reactions for the preparation of porous carbides.[17]

Generally, the low, maximum attainable[18] specific surface area has limited the application of carbides as catalyst carriers or as supports for various chemical reactions. Complicated apparatus, complex process control, and special conditions (e.g. reducing gases) are required for the reported synthetic approaches. Additionally, a very high ($>$1200 °C) temperature is a requirement for the synthesis of carbides. However, RAPET reactions are carried out under the autogenic pressure [$<$1000 psi] generated during the thermolysis of the precursor(s) in a closed reaction vessel, which induces the fabrication of carbides at much lower temperatures. In some cases, the autogenic pressure also stimulates the growth of the carbides into either rods or tubular shapes. Additionally, instead of an elemental reaction of carbon with W, Mo, or Si, individual chemical precursor(s) are chosen that contain W, Mo, or Si, carbon, oxygen, and hydrogen. Since the precursor possesses additional hydrocarbons, the reducing gases/agents are not supplied at high temperature during the carbide synthesis. More interestingly, carbides are formed as a result of the thermal dissociation of the precursor(s), which yields nanosized carbides.

---

[a] Center for Advanced Materials and Nanotechnology, Department of Chemistry, Bar-Ilan University,
Ramat-Gan 52900, Israel
E-mail: vilaspol@gmail.com
[b] Argonne National Laboratory,
Argonne, IL 60439, USA

This microreview discusses the fascinating synthesis of various carbides of silicon, tungsten, and molybdenum at a relatively low temperature by using the RAPET (Reactions under Autogenic Pressure at Elevated Temperature) approach. The solvent-, template-free, competent and straightforward RAPET process was used to synthesize a range of new carbide materials with or without the use of catalysts. Two representative examples for the synthesis of silicon, tungsten, and molybdenum carbides are presented. The ability to fabricate nanoparticles, nanorods, and nanotubes of different carbides in a one-pot reaction is also demonstrated. The thermolysis of triethylsilane afforded a high-surface area β-SiC–carbon nanocomposite and β-SiC (6–10 nm), depending upon the reaction temperatures. As an alternative to high-cost triethylsilane, a cheap precursor, silicone oil, dissociated thermally in a closed reactor that yielded nanorods of SiC with the highest surface area (563 m^2/g), could store approximately 2 wt.-% H_2 at room temperature and 6 MPa. Either micro- or nanosized spheres of Mo_2C were fabricated, depending upon the thermally dissociated starting precursor(s) in a closed reactor in an inert atmosphere at elevated temperature. The significant synthesis of WC nanotubes with a 30–60 nm diameter and a length of 1 to 10 µm is also accomplished by the direct pyrolysis of $W(CO)_6$ in the presence of Mg in a closed reactor at 900 °C. Nanoplatelets of WC are fabricated by the direct pyrolysis of a composite hybrid of 12-phosphotungstic acid ($H_3PW_{12}O_{40}$) and hexadecyltrimethylammonium bromide [$C1_6H_{33}N(CH_3)_3Br$, CTAB] in a specially designed reactor.

Experimental System for “RAPET” Reactions

The fundamental instrumentation required for RAPET reactions includes a reactor made up of stainless steel [SS], Swagelok union parts, a tubular heating furnace, an inert glove box system, and a mechanical device for opening and closing the SS reactor. As the SS parts can corrode after heating to a temperature greater than 700 °C, a reactor made up of a Haynes 230 alloy is recommended for the multiple use of the process reactor. The fabrication of various carbide nanostructures is carried out as follows. The chemical precursor(s) are introduced into a 5 mL closed reactor assembled from SS parts. The SS reactor is assembled by closing one end with a cap, after which the precursors are introduced into the reactor at room temperature under a nitrogen-filled glove box to avoid oxygen interference. The partially filled SS reactor is closed tightly by the cap at the other end, and then it is placed inside an iron pipe in the middle of the furnace for optimal heating. The temperature is raised at a rate of 10–40 °C/min to the desired/required temperature and maintained for an optimized time. The chemical dissociation and transformation reaction takes place under the autogenic pressure of the precursor at a certain temperature, followed by the gradual cooling of the reactor to room temperature. Finally, the reactor is opened, the products are collected, and a systematic compositional, morphological and structural characterization is carried out. An overview of the reactor, assembled by using Swagelok parts, is demonstrated elsewhere.[19]

Dr. Vilas G. Pol received his M.Sc. and M.Phil. degrees in chemistry from University of Pune, India. He received his Ph.D. from the Nanocenter of Bar-Ilan University, Israel, under Prof. Aharon Gedanken. After a first postdoc with Prof. Arie Zaban in dye-sensitized solar cells, he joined Dr. P. Thiyagarajan at Argonne National Laboratory, USA. Since 2002, he has published more than 70 research articles in refereed international scientific journals. Vilas has written three journal reviews and three book chapters and has filed three US patents. Vilas is an editorial board member of “Carbon Science & Technology” as well as “The Open Colloid Science Journal”. Vilas is a recipient of Intel Student Prize, Best Student Award, as well as “Gold Medal” of DRDO Sports Board, India. Recently, Vilas became an Argonne Scholar at Argonne National Laboratory, USA. Currently, he is pursuing his scientific career with distinguished scientist Michael M. Thackeray and fabricating fascinating nanomaterials for their application in energy storage and energy conversion systems.

Dr. Swati Vilas Pol obtained her M.Sc. degree in physical chemistry from University of Pune, India. She completed her Ph.D. under the supervision of Prof. Aharon Gedanken at the Center for Advanced Materials and Nanotechnology, Bar-Ilan University, Israel. She has published more than 34 scientific articles and filed one US patent. Swati is a “Meritorious student” in Maharashtra Talent Search Examination and Bharati University Scholar. Swati is currently pursuing postdoctoral research in APS at Argonne National Laboratory. Her research is based on using hard x-ray non-resonant inelastic scattering (IXS) to perform in situ studies of the core-shell electronic properties of light elements (Li, C, O) at the graphite and the lithium/metal-oxide electrode in an operating electromechanical cell, specifically a Li-ion battery.

Prof. Aharon Gedanken obtained his M. Sc. from Bar-Ilan University, and his Ph. D. degree from Tel Aviv University, Israel. After his postdoc. at USC in Los Angeles, he returned to Bar-Ilan in 1975 as a senior faculty. He has published more than 500 scientific papers in peer-reviewed journals. Professor Gedanken also filed more than 15 US patents. Prof. Gedanken is a group leader of 20 researchers which includes students, postdocs, and scientists.

The considerable advantages of the RAPET method for the synthesis of a variety of fascinating carbide nanomaterials [NMs] are: (1) It is a simple, non-aqueous, template-, surfactant-, and solvent-free method for the production of pure crystalline products. (2) Due to the closed system, it is reproducible and has easy cycleability. (3) It is an efficient and non-firing reaction, and is therefore safe. (4) The RAPET method is also applicable to highly reactive, hazardous, or carcinogenic materials (e.g. carbonyls). (5) RAPET fabricates a wide range of NMs such as metals, oxides, carbides, sulfides, phosphides, and carbonaceous materials or their core-shell morphologies. The enormous advantages and comparatively negligible limitations of the RAPET method have earned it a place as a synthetic technique in the exciting nano field. All these advantages led us to implement this innovative RAPET approach to fabricate various carbides at low temperature, in order to understand the mechanism of their formation and to study their advanced properties.

Synthesis of SiC, Mo_2C, and WC Nanomaterials

This section is divided into three major parts, namely the synthesis of SiC, Mo_2C, and WC nanomaterials. Each part describes two dissimilar ways to prepare unusual nanostructures and discusses their fascinating properties.

Synthesis of SiC Nanoparticles and Nanorods

The cracking/dissociation of a triethylsilane precursor in a 5 cm^3 closed reactor, made up of a Haynes 230 alloy at 800 °C for 3 h, yielded a (silicon carbide)–carbon nanocomposite [SCCN]. With the increase in reaction temperature to 1000 °C, more hydrocarbons were liberated that yielded SiC nanoparticles within 3 h.[20] Both reactions took place at the generated autogenic pressure of the precursor at elevated temperature in a closed reactor. The following reactions were proposed for the fabrication of SCCN and SiC at 800 °C and 1000 °C, respectively, during the controlled thermolysis of triethylsilane, without using a solvent or a catalyst. After dissociating the $C_6H_{16}Si$ precursor thermally in a closed reactor, the C and Si segregate to produce a nanosized, high-surface-area SiC in the reducing (H_2/ C_xH_y) atmosphere.

$$C_6H_{16}Si \xrightarrow{800\,^\circ C} SiC\,(s) + 2C\,(s) + nH_2\,(g) + \text{Hydrocarbons}\,(g)$$

$$C_6H_{16}Si \xrightarrow{1000\,^\circ C} SiC\,(s) + nH_2\,(g) + \text{Hydrocarbons}\,(g)$$

The irregular porous structures with 2–4 nm diameter pores are observed in the TEM of the SCCN (Figure 1a). HR-TEM analysis revealed the crystalline nature of the pore walls. The X-ray diffraction pattern of the SCCN matches the major peaks and their intensities, corresponding to carborundum (β-SiC, PDF No. 75–0254). The SCCN contains extra carbon in addition to the SiC. The presence of amorphous carbon is detected by the broad background in the XRD pattern and by EDX (energy-dispersive X-ray spectrometry) and elemental analyses. A similar XRD pattern was obtained for the activated carbon coated with silicon carbide.[21] EDX detected 1:3 atomic ratios of Si to C in the SCCN. This ratio indicates that the carbon percentage is more than sufficient to have a SiC (1:1) stoichiometry in the SCCN. The elemental analysis also measured 43% carbon in SCCN. With the increase in the reaction temperature to 1000 °C/3 h, crystalline SiC with an approximately 6 nm particle diameter is obtained without excess carbon (Figure 1b). The measured distance between the (111) lattice planes is 0.251 nm, which is very close to the distance between the planes reported in the literature (0.252 nm) for the face-centered cubic lattice of SiC.

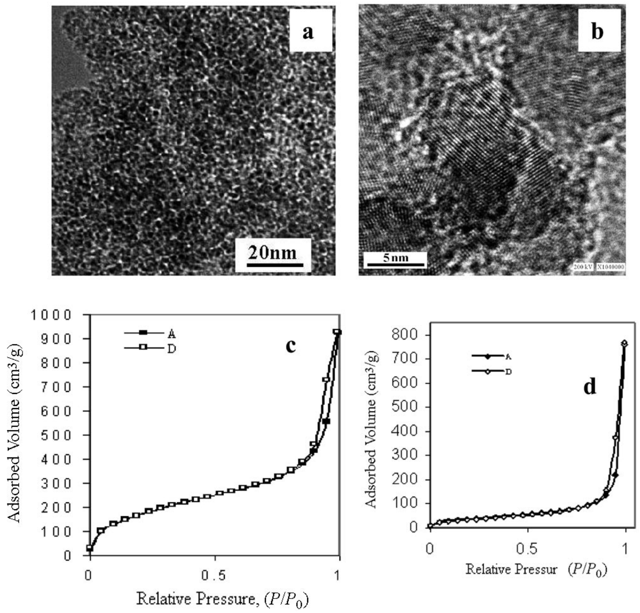

Figure 1. Transmission electron micrographs of (a) SCCN prepared at 800 °C, (b) SiC prepared at 1000 °C, and N_2 adsorption/desorption isotherms of the (c) SCCN and (d) SiC samples.

Figure 1c shows the N_2 adsorption-desorption isotherms of the SCCN sample that was prepared at 800 °C. The isotherm exhibits an abrupt change when the relative pressure is greater than 0.9, indicating that the sample possesses a porous[22] structure. The calculated BET surface area is 656 m^2/g, and a large pore volume of 0.588 cm^3/g is recorded. It is worth noting that in addition to silicon carbide we have bare carbon (ca. 50%), which might cause the high surface area. Atwater[21] et al. reported a surface area of 1263 m^2/g for the activated carbon coated with silicon carbide. The measured surface area of the SiC sample prepared at 1000 °C is 149 m^2/g (Figure 1d), and the sample has a larger pore volume of 0.683 cm^3/g. This sudden drop/reduction in the surface area, as compared with SCCN, is due to the consumption of bare carbon to form hydrocarbons that are released as gases. However, this value is higher than that previously reported.[23] The BJH (Barrett–Joyner–Halenda) method[24] was employed to calculate the pore size distribution of the SiC and SCCN samples. Pore size distributions for SCCN and SiC samples covered pore diameters ranging between 40 and 380 Å. The distribution of pore sizes in both the SCCN and SiC samples shows that the percentage of the large pore diameters is more than 70%.

Here, at a relatively low temperature, we synthesized high-surface-area, nanosized SiC or SCCN by using a single triethylsilane precursor with the efficient RAPET technique. Although we could achieve SiC from the thermolysis of triethylsilane, the precursor is highly expensive and not environmentally friendly. We continued our efforts to produce SiC by employing the RAPET technique by using other precursors. The vinyltrimethylsilane also produced analogous silicon carbides. Considering the high cost of organosilanes for the fabrication of high-surface-area SiC nanorods, we have discovered an alternative, environmentally friendly, and cheaper precursor, silicone oil. The thermolysis of commercial silicone oil at a relatively low temperature, (800 °C)/3 h, in a closed reactor yielded high-surface-area (563 m^2/g) β-SiC nanorods.[25] The XRD diffraction pattern of the SiC nanorods is in agreement with the diffraction peaks, peak intensities, and cell parameters of crystalline fcc β-SiC (PDF No. 73–1665.)

The commercial silicone oil is composed of the elements C, H, O, and Si. The carbon, hydrogen, and sulfur contents in the reactant (commercial silicone oil) and the formed product (SiC nanorods) were measured by elemental analysis (Eager 200). The elemental analysis of the commercial silicone oil showed the presence of only carbon and hydrogen. The analysis measured 32.8% carbon and 8.2% hydrogen in the commercial silicone oil. This confirms the purity of silicone oil and the absence of a sulfur impurity. The carbon content in the product (SiC nanorods) is 24.9%, which matches well with that of the SiC powder (26%) received from Alfa-Aesar. The measured amount of hydrogen in SiC nanorods is 0.6%. The energy-dispersive X-ray analysis showed a 1:1 molar ratio of Si to C. EDS (energy-dispersive spectrometry) also detected a small amount of oxygen ($<1\%$) in the product. The oxygen contamination in SiC nanorods was also measured by an oxygen analyzer (Eager 200) and was found to be 0.6 atom.-%. For comparison, we used Alfa-Aesar SiC material that showed 0 atom.-% of oxygen. Thermogravimetric analysis of SiC nanorods was carried out under a flow of air in the temperature range 25–900 °C in order to study the weight loss/gain with an increase in temperature. It is observed from the TGA curve that there is almost no drastic gain or loss of weight in the SiC nanorod sample in the temperature range 25–800 °C. A slight (ca. 4%) weight loss was observed above 800 °C. The analogous TGA curve is obtained for the Alfa-Aesar SiC sample. This confirms the purity of the formed SiC nanorods. By taking advantage of the achieved higher surface area of SiC nanorods, the possibility of hydrogen storage is tested for the first time. Interestingly, the β-SiC nanorods with a diameter of approximately 50 nm and lengths of more than micrometers can adsorb approximately 2 wt.-% H_2 at room temperature and 6 MPa.

Figure 2a shows a SEM image of SiC nanorods, prepared by the thermal decomposition of silicone oil, having a diameter of approximately 50 nm and a length of more than 1 μm. The inserted SEM image of a single straight SiC nanorod shown at high resolution presents a diameter of approximately 75 nm and a length of 1 μm with a smooth surface. The as-grown SiC nanorods are crystalline fcc β-SiC, as confirmed by XRD. Further processing is therefore not required. The EDX analysis (attached to a JEOL-JSM 840 scanning electron microscope) also revealed a 1:1 molar ratio of Si to C. The HR-TEM on the edge of a single nanorod is depicted in Figure 2b, which provides further evidence for the identification of the product as SiC. It illustrates the perfect arrangement of the atomic layers with minimum defects. The measured distance between these (111) lattice planes is 0.253 nm, which is very close to the literature value (0.2516 nm) for the face-centered cubic lattice of SiC (PDF: 73–1665). The stability of the SiC nanorods was studied by employing thermogravimetric analysis under a flow of air, which does not show any drastic weight gain or loss in a temperature range of 25 to 800 °C.

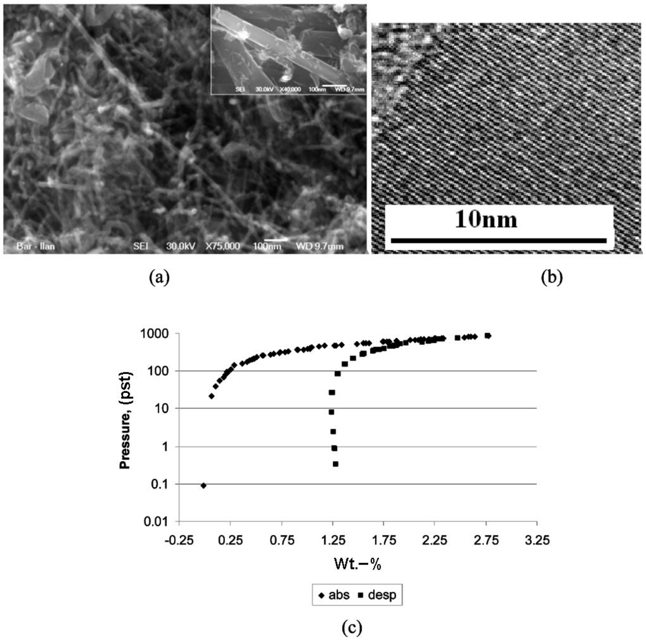

Figure 2. The (a) SEM and (b) HR-TEM of SiC nanorods. (c) Room temperature H_2 storage in SiC nanorods.

The probable reactions involved in the formation of the SiC nanorods from poly(dimethylsiloxane)/silicone oil are as follows. Within one hour, SiO and carbon are the multiproducts obtained. Thus, we continued the reaction up to 3 h, obtaining SiC nanorods as the sole product. In another control experiment where the polymeric precursor was directly heated in a furnace in an inert atmosphere, most of the hydrocarbons from the silicone oil were released and favored the fabrication of submicron sized amorphous silica. However, the RAPET reaction in a closed system in an inert environment favors the fabrication of SiC nanorods. This means that the isolated hydrocarbons act as a continuous reducing environment at high temperature to favor the fabrication of crystalline SiC instead of silica. This confirms that an autogenic pressure in the RAPET reaction plays an important role and facilitates the fabrication of SiC nanorods, even at 800 °C.

$$(\text{–}SiC_2H_6O\text{–})_n \xrightarrow{800\,°C/1h} SiO + 2C + 3H_2 \xrightarrow{800\,°C/3h} SiC\ (s) + CO\ (g)$$

A similar type of reaction is also reported by Rao[26] et al. for the formation of SiC nanowires by heating silica gel with activated carbon at 1360 °C under a H_2 or NH_3 atmosphere.[26] The SiC nanorods appear to be straight or wire-like, and they seem to grow out of the carbon–silica composite particles. Our present reaction occurred at a relatively low temperature (800 °C) as it was carried out under the autogenic pressure created during the thermolysis of the precursor.

The BET surface area is 563 m^2/g, and a pore volume of 0.0132 cm^3/g is measured for the SiC nanorods. Indeed, this is a very high surface area for the carbide material. Therefore, the hydrogen take-up by these high-surface-area SiC nanorods is measured. The measurement was performed on a commercial pressure-composition (P-C) isotherm unit (Advanced Materials), as described previously.[27] The silicon carbide nanorods with a diameter of approximately 50 nm and lengths of more than micrometers can adsorb 2.5 wt.-% H_2 at room temperature and 6 MPa (Figure 2c). However, the adsorption and desorption curves do not meet when the pressure is lowered to an ambient level. Only approximately 1.5wt.-% H_2 can be reversibly absorbed and released. This suggests some chemisorption of H_2 on SiC nanorods, which may be responsible for the irreversible nature of the room-temperature adsorption. Furthermore, we continued to implement the RAPET approach to fabricate Mo_2C, either in micro or nano size.

Synthesis of Mo_2C Micro- and Nanospheres

To fabricate micron-sized Mo_2C, mesitylene (C_9H_{12}) was treated with $Mo(CO)_6$ at 700 °C under inert atmosphere in a closed reactor, which led to the fabrication of approximately 2 µm spherical bodies.[28] These bodies are identified as hexagonal (space groups: *P*6_3*/mmc*) α-Mo_2C by XRD measurement (Figure 3a). To fabricate nanosized Mo_2C, the thermal decomposition of molybdenum 2-ethylhexanoate at 700 °C under an inert atmosphere, which yielded 30 nm particles of α-Mo_2C, was confirmed by XRD measurements (Figure 3b).

The TEM of Mo_2C (Figure 3c) shows approximately 2 µm spherical bodies with very smooth surfaces. If we mix a precursor without metal (hydrocarbons such as C_9H_{12}) and an organometallic precursor, $Mo(CO)_6$, we still get microspheres in the product. On the contrary, the formation of nanosized carbides is obtained by the decomposition of only an organometallic precursor. Thus, the precursor requires the presence of the metal as a self-catalyzing element to yield a nanosized product. The thermal decomposition of molybdenum 2-ethylhexanoate produced approximately 50 nm spherical particles of α-Mo_2C. The insert in Figure 3d shows that the Mo_2C particles are 30–50 nm in diameter. The possible explanation for the micron size of the noncatalytic static process (vs. the catalytic one or the higher temperature flow process) relates to nucleation rates. If nucleation is rapid (catalyst or high temperaure), then one obtains many small spheres. If nucleation is slow (relative to growth), then one gets larger spheres. The production of distinct, non-agglomerated spheres suggests a gas-to-particle (or gas-to-droplet) conversion process. If this were an all-condensed-phase process, one would typically obtain a monolithic product, not the separate spheres. A detailed explanation on micro vs. nano formation of Mo_2C is presented elsewhere.[28] Apart from the synthesis and morphology of traditional carbides, we chose to synthesize WC in the tubular or rod-shaped morphology. Before our report on WC nanotubes, the tubular morphology for WC was unknown in the literature. To the best of our knowledge, this is the first report where the nanotubes of WC have been fabricated by employing RAPET techniques.

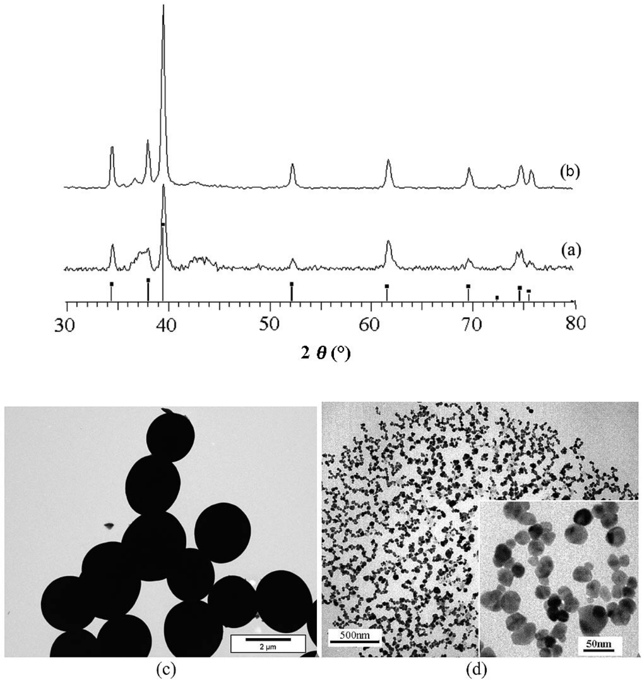

(c) (d)

Figure 3. XRD patterns of α-Mo_2C obtained after the thermal decomposition of: (a) the product obtained after thermolysis of a mixture of $Mo(CO)_6$ with mesitylene (C_9H_{12}); (b) molybdenum 2-ethylhexanoate. TEM of (c) the product obtained after thermolysis of a mixture of $Mo(CO)_6$ and mesitylene and (d) the decomposed product of molybdenum 2-ethylhexanoate.

Synthesis and Electrochemical Properties of WC Nanotubes

In a typical synthesis of WC nanotubes, 820 mg of $W(CO)_6$ and 410 mg of pure Mg powder were used. At a relatively low temperature (900 °C), the thermal decomposition of $W(CO)_6$ in the presence of low melting- and boiling point Mg powder is carried out under its autogenic pressure in a closed reactor to fabricate the nanotubes of WC and MgO nanoparticles,[29] as shown in Figure 4a. The magnesia contamination was dissolved in a 30% dilute HCl solution, washed three times with anhydrous ethanol, centrifuged at 9000 rpm, and vacuum dried for 12 h. The dried product indexed to the hexagonal phase (space group *P6m2*) with lattice constants a = 2.90 Å and c = 2.83 Å of WC (peak intensities and positions match with PDF No. 51–939). The thermal decomposition of bare $W(CO)_6$ yields a mixture of WO_2, WC, W_2C and C, exhibiting the growth tendency.[29] In an attempt to remove the O from WO_2, we performed several control experiments at different temperatures in the 800 to 950 °C range. WO_2 is the predominant product at 800 °C, 900 °C, and even at 950 °C when the reactants were H_2WO_4 + Mg and WO_3 + Mg + C. In addition, the morphology of the product remains a mixture of particles and short wires. With a longer reaction time (8 h) at 900 °C, the length of the wires could increase up to 1 μm, maintaining analogous reaction products such as WO_2, WC, W_2C, and C. In the present $W(CO)_6$ system [reaction (1)], the reason for the addition of Mg is to use its reactivity with oxygen, thereby avoiding the formation of WO_2. Indeed, the reaction products are WC + MgO + W_2C + C [reaction (3)]. On the basis of previous findings and the control reactions; we suggest a mechanism for the formation of WC given by reactions (1) to (5).

$$W(CO)_6 \rightarrow W + 6CO \tag{1}$$

$$W + 2CO \rightarrow WO_2 + 2C \tag{2}$$

$$WO_2 + 2Mg \rightarrow W + 2MgO \tag{3}$$

$$2CO \rightarrow C + CO_2 \text{ (Boudard reaction)} \tag{4}$$

$$W + C \rightarrow C + W_2C \tag{5}$$

The final products, WC and W_2C, are obtained in reaction (5), and carbon is obtained in reactions (2) and (4). Whether MgO catalyzes reaction (5) is not yet clear. The present reaction is complex because CO might undergo disproportionation (Boudard reaction) to produce CO_2 and carbon (reaction 4). It is likely that Mg promotes the CO dissociation reaction in a similar manner, as in the case of the alkali-promoted Fischer–Tropsch catalysis.[30] Finally the directed growth of hexagonal WC unit cells in a very specific direction[29] in the presence of MgO yields WC tubes.

The WC nanotubes obtained after HCl treatment possess diameters ranging from 30 to 70 nm and lengths varying from 1 to 10 μm. EDX analysis carried out on the bulk WC nanotubes shows a 1:1.07 molar ratio for W/C. The WC nanotubes are free of MgO particles, as shown in the TEM in Figure 4b. The insert image shows a typical WC nanotube coil having a diameter of 70 nm and a length of more than a micrometer.

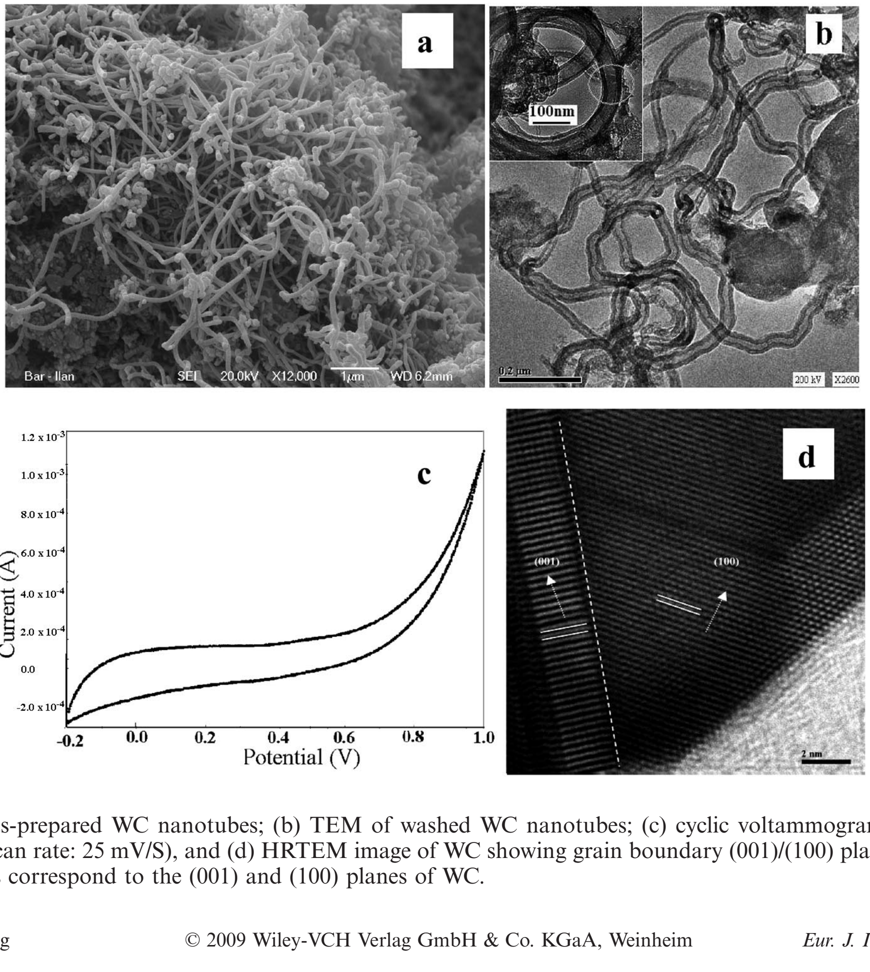

Figure 4. (a) SEM of as-prepared WC nanotubes; (b) TEM of washed WC nanotubes; (c) cyclic voltammogram of WC nanotubes in 0.5 M of sulfuric acid (scan rate: 25 mV/S), and (d) HRTEM image of WC showing grain boundary (001)/(100) planes marked with dotted lines. The lattice fringes correspond to the (001) and (100) planes of WC.

The electrochemical stability of WC nanotubes was measured in 0.5 M H_2SO_4 by using a WC-coated glassy carbon electrode employed as a working electrode. Figure 4c shows the cyclic voltammogram of WC nanotubes after the steady-state condition. The voltammogram showed a large current increase above 0.6 V, indicating the oxidation of WC. In the reverse scan, there was a cathode current due to the reduction of the oxidized species during the anodic scan. Similar electrochemical stability for WC nanorods is reported by Shan et al. They produced WC nanorods and nanoplatelets by the direct pyrolysis of a composite hybrid of 12-phosphotungstic acid ($H_3PW_{12}O_{40}$) and hexadecyltrimethylammonium bromide [$C1_6H_{33}N(CH_3)_3Br$, CTAB] in a specially designed RAPET reactor.[31] The diameters of the WC rods are 30–50 nm with varying lengths of 600–1000 nm, and the sizes of the platelets are around 55 nm. The high-resolution TEM micrographs clearly indicate that the rod is highly crystalline in nature (Figure 4d). The HRTEM illustrates that the platelet consists of surface features such as steps, kinks, and terraces. It shows the lattice fringes with a spacing of $d = 0.252$ nm, which closely matches the (100) plane of hexagonal WC.

With our understanding of the low-temperature carbide synthesis by the RAPET technique, it is anticipated that a facile RAPET synthesis approach can be extended to the preparation of other carbides, such as vanadium carbide (V_8C_7), titanium carbide (TiC), iron carbide, ZrC, Al_4C_3, etc. Additionally, these carbides can find application as a catalyst support or even in hydrogen storage.

Summary

The solvent-, template-free, competent, straightforward, and scalable RAPET process was used to synthesize novel nanoparticles, nanorods, or nanotubes of carbides. The experimental results showed that β-SiC nanoparticles (6–10 nm) with approximately 150 m^2/g were produced by the single-step thermolysis of triethylsilane at 1000 °C in a closed reactor. Silicone oil is proposed as the alternative to high-cost triethylsilane. Thermally dissociated silicone oil, which yielded nanorods of SiC with highest surface area (563 m^2/g), could store approximately 2 wt.-% of H_2 at room temperature and 6 MPa. Depending on the thermally dissociated starting precursor(s), either micro- or nanosized Mo_2C spheres are fabricated in a closed reactor in an inert atmosphere at elevated temperature. The 30–60 nm diameter WC nanotubes with a length of more than a few micrometers are prepared by the direct pyrolysis of $W(CO)_6$ in the presence of Mg powder in a closed reactor at 900 °C. The fabrication of various carbides at much lower temperatures is accomplished in RAPET reactions as a result of the autogenic pressure created during the thermolysis of the precursor(s). In the RAPET process, the reducing gases/agents are not additionally supplied during the synthesis of nanosized silicon, tungsten, and molybdenum carbides.

---

[1] C. Zollfrank, H. Sieber, *J. Am. Ceram. Soc.* **2005**, *88*, 51–58.
[2] J. Fan, X. Wu, H. Li, H. Liu, G. Siu, K. Chu, *Appl. Phys. Lett.* **2006**, *88*, 41909 (1–3).
[3] X. Deng, N. Chawla, K. Chawla, M. Koopman, J. Chu, *Adv. Eng. Mater.* **2005**, *7*, 1099–1108.
[4] A. Muller, P. Gerstel, E. Butchereit, K. Nickel, F. Aldinger, *J. Eur. Ceram. Soc.* **2004**, *24*, 3409–3417.
[5] R. B. Levy, M. Boudart, *Science* **1973**, *181*, 547–548.
[6] S. B. Qadri, M. A. Imam, C. R. Feng, B. B. Rath, M. Yousuf, S. K. Singh, *Appl. Phys. Lett.* **2003**, *83*, 548–550.
[7] G. W. Meng, L. D. Zhang, C. M. Mo, S. Y. Zhang, Y. Qin, S. P. Feng, H. J. Li, *J. Mater. Res.* **1998**, *13*, 2533–2538.
[8] I. N. Kholmanov, A. Kharlamov, E. Barborini, C. Lenardi, B. A. Li, C. E. Bottani, C. Ducati, S. Maffi, N. V. Kirillova, P. Milani, *J. Nanosci. Nanotechnol.* **2002**, *2*, 453–456.
[9] J. M. Nhut, R. Vieira, L. Pesant, J. P. Tessonnier, N. Keller, G. Ehret, C. Pham-Huu, M. J. Ledoux, *Catal. Today* **2002**, *76*, 11–32.
[10] N. Keller, C. Pham-Huu, G. Ehret, V. Keller, M. J. Ledoux, *Carbon* **2003**, *41*, 2131–2139.
[11] G. Z. Shen, D. Chen, K. B. Tang, Y. T. Qian, S. Y. Zhang, *Chem. Phys. Lett.* **2003**, *375*, 177–184.
[12] F. H. Ribeiro, R. A. Dalla Betta, G. Y. Guskey, M. Boudart, *Chem. Mater.* **1991**, *3*, 805–812.
[13] G. L. Tan, C. H. Chen, S. C. Cheang, K. M. Uang, *Appl. Phys. Lett.* **2004**, *85*, 2358–2360.
[14] J. M. Girandon, P. Devassine, J. F. Lamonier, L. Delannoy, L. Lecleveq, G. Leclereq, *J. Solid State Chem.* **2000**, *154*, 412–426.
[15] P. N. Ross, P. Stonehart, *J. Catal.* **1975**, *39*, 298–301.
[16] ^{1}.-P. Ying, C. Li, *Chem. Mater.* **2002**, *14*, 3148–3151.
[17] S. T. Oyama, *The Chemistry of Transition Metal Carbides and Nitrides*, Blackie Academic & Professional, London, U. K., **1996**.
[18] C. H. Liang, G. W. Meng, L. D. Zhang, Y. C. Wu, Z. Cui, *Chem. Phys. Lett.* **2000**, *329*, 323–328.
[19] S. V. Pol, V. G. Pol, A. Gedanken, *Chem. Eur. J.* **2004**, *10*, 4467–4473.
[20] V. G. Pol, S. V. Pol, A. Gedanken, *Chem. Mater.* **2005**, *17*, 1797–1802.
[21] J. E. Atwater, J. R. Akse, T. C. Wand, S. Kimura, D. C. Johnson, *Chem. Eng. Sci.* **2001**, *56*, 2685–2693.
[22] J. Guo-Qiang, G. Xiang-Yun, *Microporous Mesoporous Mater.* **2003**, *60*, 207–212.
[23] J. Parmentier, J. Patarin, J. Dentzer, C. Vix-Gutlerl, *Ceram. Int.* **2002**, *28*, 1–7.
[24] E. P. Barret, G. Joyner, P. P. Halenda, *J. Am. Chem. Soc.* **1951**, *73*, 373.
[25] V. G. Pol, S. V. Pol, A. Gedanken, S. H. Lim, Z. Zhong, J. Lin, *J. Phys. Chem. B* **2006**, *110*, 11237–11240.
[26] G. V. G. Gundiah, A. Madhav, M. D. Govindaraj, M. Seikh, C. N. R. Rao, *J. Mater. Chem.* **2002**, *12*, 1606–1611.
[27] S. H. Lim, J. Luo, Z. Zhong, W. Ji, J. Lin, *Inorg. Chem.* **2005**, *44*, 4124–4126.
[28] V. G. Pol, S. V. Pol, J. M. Calderon Moreno, A. Gedanken, *Carbon* **2006**, *44*, 3285–3292.
[29] S. V. Pol, V. G. Pol, A. Gedanken, *Adv. Mater.* **2006**, *18*, 2023.
[30] S. J. Jenkins, D. A. King, *J. Am. Chem. Soc.* **2000**, *122*, 10610–10614.
[31] S. Shanmugam, D. S. Jacob, A. Gedanken, *J. Phys. Chem. B* **2005**, *109*, 19056–19059.

Received: October 22, 2008